Patient Safety Starts Here

"If you were to purchase a 3D Scanning System today, which would you choose?"

When asked this question by a 2016 MEDPHYS Mailing List survey, the majority of respondents chose the 3D SCANNER™ from Sun Nuclear. More than 550 facilities worldwide agree—the 3D SCANNER is their preferred water tank for accurate and efficient commissioning.

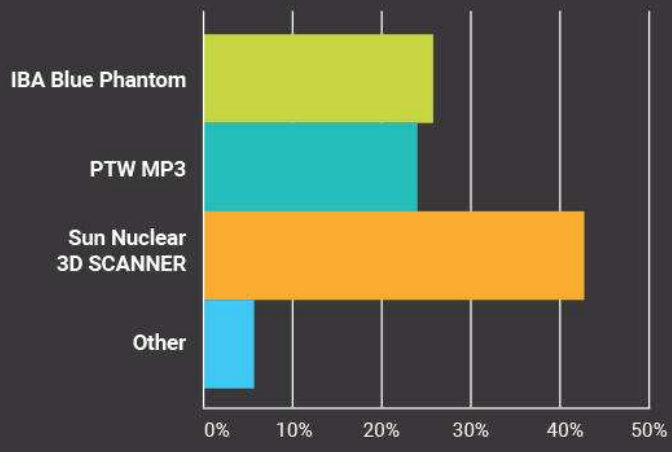

Visit sunnuclear.com to learn about these advantages and more.

SUN NUCLEAR corporation

© 2017 Sun Nuclear Corporation. All rights reserved.

Evaluation of the gamma dose distribution comparison method

Daniel A. Low[a)]
Department of Radiation Oncology, Washington University School of Medicine, St. Louis, Missouri 63110

James F. Dempsey
Department of Radiation Oncology, University of Florida, Gainesville, Florida 32610

(Received 19 March 2003; revised 18 June 2003; accepted for publication 19 June 2003; published 22 August 2003)

The γ tool was developed to quantitatively compare dose distributions, either measured or calculated. Before computing γ, the dose and distance scales of the two distributions, referred to as evaluated and reference, are renormalized by dose and distance criteria, respectively. The renormalization allows the dose distribution comparison to be conducted simultaneously along dose and distance axes. The γ quantity, calculated independently for each reference point, is the minimum distance in the renormalized multidimensional space between the evaluated distribution and the reference point. The γ quantity degenerates to the dose-difference and distance-to-agreement tests in shallow and very steep dose gradient regions, respectively. Since being introduced, the γ quantity has been used by investigators to evaluate dose calculation algorithms, and compare dosimetry measurements. This manuscript examines the γ distribution behavior in two dimensions and evaluates the γ distribution in the presence of data noise. Noise in the evaluated distribution causes the γ distribution to be underestimated relative to the no-noise condition. Noise in the reference distribution adds noise in the γ distribution in proportion to the normalized dose noise. In typical clinical use, the fraction of points that exceed 3% and 3 mm can be extensive, so we typically use 5% and 2–3 mm in clinical evaluations. For clinical cases, the calculation time is typically 5 minutes for a 1×1 mm^2 interpolated resolution on an 800 MHz Pentium 4 for a 14.1×15.2 cm^2 radiographic film. © *2003 American Association of Physicists in Medicine.*
[DOI: 10.1118/1.1598711]

Key words: radiation therapy, intensity modulated radiation therapy, dose distribution comparison, gamma tool

I. INTRODUCTION

The clinical utilization of intensity modulated radiation therapy (IMRT) has lead to the widespread need for multidimensional dose distribution measurements and comparisons. To provide quantitative measurements, multidimensional dosimeters such as radiochromic film[1–6] and polymerizing gels[7–14] have been developed. One of the difficulties with using these, or other multidimensional dosimeters is the large amount of measurement data that has to be analyzed and compared. Typically evaluations of dose measurements include comparison with either other measurements (e.g., using other dosimeters) or, more commonly, against calculated dose distributions. Dose comparison tools have been developed to aid such comparisons.[15–18] For purposes of this paper, dose comparisons will be between two distributions, termed the reference and evaluated distributions. The labels are necessary because some of the tools are not symmetric with respect to which distribution is selected for each role. As envisioned in this work, the reference distribution will typically be a measurement benchmark to which a calculated, evaluated, distribution will be compared. This means that the dimensionality of the reference distribution will usually be smaller than or the same as the evaluated distribution.

The dose comparison test suite has typically included the dose difference test, where the numerical dose difference is computed, point-by-point, using local spatial interpolation if necessary to co-locate the evaluated dose distribution and the reference distribution. A limitation with the dose-difference test is that it becomes overly sensitive in steep dose gradient regions. For example, small spatial offsets between the two distributions caused by experimental measurement error yield otherwise identical dose distributions to exhibit large dose differences in regions of steep dose gradients. Therefore, the usefulness of the dose difference test is strongest in regions of relatively shallow dose gradients. Displays of dose-difference distributions are typically marked by numerically large values in regions of steep dose gradients for the reasons mentioned above. Determining in which regions the dose differences are significant may require a point-by-point manual evaluation of the local dose gradient. The dose difference tool is anti-symmetric with respect to which distribution is selected as the reference distribution.

The sensitivity of the dose difference tool to steep dose gradients led to the development of the distance-to-agreement (DTA) tool.[15,17] This tool, as interpreted in this paper, is applied to the evaluated distribution independently for each reference point. For a specific reference point, the evaluated dose distribution is searched to locate the nearest point with the same dose value, equivalent to locating the closest approach of the isodose line or surface in the evaluated distribution corresponding to the same dose as the reference point. For discretized dose distributions, spatial inter-

polation is generally required to determine the minimum distance. Unlike the dose difference tool, the DTA tool is not overly sensitive in steep-dose gradient regions. However, in shallow dose gradient regions, a large DTA value may be computed even for relatively small dose differences. Because steep dose gradient regions are typically much smaller in size than shallow dose gradient regions, much of DTA distributions will exhibit regions of disagreement greater than the clinically acceptable criterion. This feature makes DTA distributions very difficult to visually interpret. The DTA tool is neither antisymmetric nor invariant with respect to which distribution is selected as the reference distribution. Both dose difference and DTA analyses provide continuous distributions that can be displayed to the reviewer, for example as a colorwash, or summarized in a histogram.

Because of the complementary sensitivity of these tests, a combined test was developed, termed the composite distribution.[15,19,20] The composite distribution identifies regions where the dose-difference and DTA are simultaneously greater than pre-selected clinical criteria. In principal, regions where one test is overly sensitive will be the same region that the complementary test is appropriately sensitive, so failure by both criteria indicates that the two distributions disagree in a clinically significant fashion.

While the composite distribution solves the difficulty with the individual tests, it has some significant limitations. The composite distribution is essentially binary, it records a pass-fail result based on the user-specified criteria for the two independent tests. Display of this distribution shows regions that fail the tests, but provides no information of the magnitude of the failure. For example, the DTA and dose differences may just exceed the tolerances, or they may exceed them by a large amount, the composite distribution will have the same value, only identifying that they failed both tests. Tabular summaries are limited to counting the points that passed and failed, although these statistics can be subdivided according to dose magnitude, dose gradient, or other quality of the dose distribution.

A generalization of the composite distribution was developed by our group (Low *et al.*[16]), termed the γ distribution, that addresses the limitations of the composite distribution. The γ distribution has been used by us and other authors to compare dose distributions.[8,21–23] The presentation in the original paper was preliminary. For example, one limitation of that paper was that the examples were shown only in one dimension. While it is perfectly acceptable to use this tool in one dimension, because of the widespread use of film-based dose distribution measurements, the testing methods are likely to be more useful in comparing distributions of two dimensions. Another limitation of the paper was that the sensitivity of the tests to noise in the dose distributions was not evaluated. This paper addresses these limitations and presents some two-dimensional examples of the use of the γ distribution.

II. METHODS AND MATERIALS

We have implemented a slight change to the previously published nomenclature.[16] The original paper specified the two distributions as "measured" and "calculated," implying that the comparisons are always made between these distributions and that the measurement is always the benchmark dataset. Because the γ tool is not symmetric with respect to the two distributions, and because either or both distribution can be measured or calculated, we now use the terms "evaluated" and "reference" to replace calculated and measured, respectively. The γ tool is calculated independently for each reference point using the entire evaluated distribution. The new nomenclature is summarized in Table I for clarity. Refer to Low *et al.*[16] for figures showing one- and two-dimensional examples of these terms.

In general, the evaluated distribution will have at least as high a dimensionality as the reference distribution. For example, the reference distribution may be a two-dimensional film dose distribution measurement, while the evaluated distribution may be a full 3D dose distribution calculation. Note that the γ function is defined independently for each reference point so the neighboring reference points do not influence the computation of γ at that point. Therefore, the reference distribution may consist of as little as a single point dose measurement. For this study, both the evaluated and reference distribution were two dimensional.

A. Square fields

To show the performance of the dose comparison tools for a case that has clinical relevance, has both steep and shallow dose gradients, and would provide a straightforward visual display of the tool's performance, we selected a projection through a 10×10 cm^2, 6 MV beam incident on a water phantom. The dose distributions were calculating using a fit to clinical data originally published by our group.[16] The extension of this model to two-dimensions yielded slight low-dose artifacts outside the beam penumbra and along the diagonal field axes, but this did not significantly affect the dose comparison tool evaluations. The dose distribution was normalized to 1.0 at the central axis, had a maximum dose gradient of 12% mm^{-1}, and for most evaluations, had a pixel spacing of 1×1 mm^2. The reference dose distribution used an unmodified version of this distribution [Fig. 1(a)]. We tested the γ function under conditions that provided discrepancies that would independently highlight the dose-difference and DTA tests using acceptance criteria of 3% and 3 mm, respectively. The square dose distribution shown in Fig. 1(a) was modified in quadrants to create the evaluated distribution. In quadrant 1, labeled unmod, the evaluated distribution was not modified, so with no added noise, the reference and evaluated dose distributions were identical. In quadrant 2, labeled dose shift, the dose was modified by providing a multiplicative dose offset that was a function of the off-axis distance x such that

$$\Delta\text{Dose}=0.012x \tag{1}$$

yielding a $\pm3\%$ dose difference (the dose difference criterion ΔD) at $x=\pm2.5$ mm, respectively. In quadrant 3, labeled space shift, the reference distribution was spatially skewed using the offset

TABLE I. Definitions of symbols used in this paper and suggested for future papers.

Symbol	Equation	Description
$D_e(\vec{r}_e)$	N/A	Evaluated dose D_e at position $\vec{r}_e$
$D_r(\vec{r}_r)$	N/A	Reference dose D_r at position $\vec{r}_r$
ΔD	N/A	Dose difference criterion. For the examples in this paper, ΔD is not a function of dose gradient, dose level, or spatial location and is selected to be 3% of the maximum dose
Δd	N/A	Distance-to-agreement criterion. For the examples in this paper, Δd is not a function of dose gradient, dose level, or spatial location and is selected to be 3 mm
$r(\vec{r}_e,\vec{r}_r)$	$r(\vec{r}_e,\vec{r}_r)=\lvert\vec{r}_e-\vec{r}_r\rvert$	Spatial distance between evaluated and reference dose points
$\delta(\vec{r}_e,\vec{r}_r)$	$\delta(\vec{r}_e,\vec{r}_r)=D_e(\vec{r}_e)-D_r(\vec{r}_r)$	Difference between evaluated dose $D_e(\vec{r}_e)$ at position $\vec{r}_e$ and reference dose $D_r(\vec{r}_r)$ at position $\vec{r}_r$
$\Gamma(\vec{r}_e,\vec{r}_r)$	$\Gamma(\vec{r}_e,\vec{r}_r)=\sqrt{\frac{r^2(\vec{r}_e,\vec{r}_r)}{\Delta d^2}+\frac{\delta^2(\vec{r}_e,\vec{r}_r)}{\Delta D^2}}$	Generalized Γ function, computed for all evaluated positions $\vec{r}_e$ and reference positions $\vec{r}_r$
$\gamma(\vec{r}_r)$	$\gamma(\vec{r}_r)=\min\{\Gamma(\vec{r}_e,\vec{r}_r)\}\forall\{\vec{r}_e\}$	γ function, the minimum generalized Γ function in the set of evaluated points

$$\Delta y = 0.12x, \tag{2}$$

where y refers to the direction perpendicular to the field edge. This produced an offset in the y direction of ± 3 mm (the DTA criterion Δd) at an off-axis distance at $x = \pm 2.5$ mm, respectively, and was used to create dose distribution discrepancies for which the DTA tool was sensitive.

Quadrant 4, labeled both, simultaneously employed both modifications [Eqs. (1) and (2)] to the reference distribution, with suitable replacement of the y-axis and x-axis variables.

To examine the influence of pixel-to-pixel noise on the dose comparison tools, pseudorandom normally distributed noise was imposed as a multiplicative factor to the reference and evaluated distributions. Noise was imposed with single standard deviations of up to 3%. For all tests, the dose-difference, distance-to-agreement, composite, and γ analyses were conducted.

B. Constant dose gradient

The tests using the dose distributions shown in Figs. 1(a) and 1(b) provided qualitative displays of the tools' performance under the influence of noise. One of the advantages of the γ distribution is that, because it provides a continuous numerical value, the γ distribution can be summarized in a histogram. The use of a histogram provides to the user an efficient summary of the quality of comparison between the two dose distributions. The user can easily identify the fraction of reference points that are within acceptable tolerances ($\gamma \leqslant 1$), as well as the fraction of reference points that do not meet the tolerances and by how much. A quantitative test was used to investigate the sensitivity and behavior of γ, and specifically for γ histograms, as a function of added noise. Dose distributions with constant, user-specified dose gradients were modeled and the pixel spacing, γ tolerance values, dose gradient, noise-free dose difference between the evaluated and reference distributions, and additive normally distributed noise were varied. The γ histograms were presented as two-dimensional distributions, with each row having a γ histogram corresponding to a separate comparison test, each with a unique additive noise standard deviation.

III. RESULTS

A. Square field

The square-field evaluation of the dose comparison tools with no added noise is shown in Fig. 1. The reference and evaluated distributions are shown in Figs. 1(a) and 1(b), respectively. The dose-difference distribution is shown in Fig. 1(c). Quadrant 1 (unmodified) shows a constant value of zero, while quadrant 2 (dose shift) shows the slowly varying dose difference. Both of these quadrants clearly reflect the differences between the reference and evaluated distributions. The dose difference in quadrant 3 (space shift) shows only small dose differences except near the beam edge, where, because of the steep dose gradient, the dose differences become large, even with only a relatively small spatial shift between the two dose distributions. This striking dose-difference feature is typical of small spatial offsets in steep

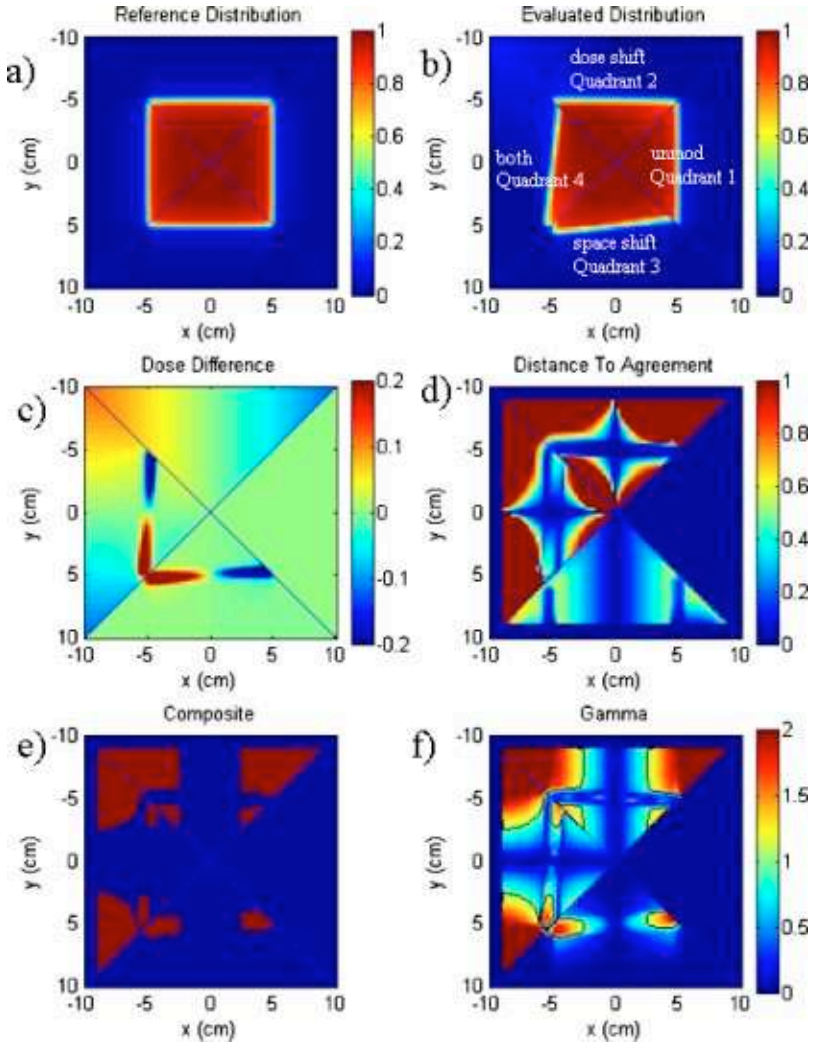

FIG. 1. Example of dose analysis tools for model and modified 10×10 cm^2 fields representing the reference and evaluated dose distributions, respectively, with no added noise. The gamma tool uses 3% and 3 mm dose difference and distance-to-agreement criteria, respectively.

dose gradient regions. Quadrant 4 (both) clearly identifies the dose shift component in both the high dose and low dose regions except when coincident with steep dose gradients, where the spatial offset causes very large dose differences.

The DTA tool is shown in Fig. 1(d) (the outer 1.0 cm are not defined because the DTA search was limited to a 1.0 $\times 1.0$ cm^2 square). There is a qualitative difference between the presentation and subsequent interpretation of the dose-difference and DTA tools. DTA distributions tend to have numerous complex features, due in part to the fact that shallow dose gradient regions extend over larger areas than steep dose gradient regions. Interpretation of the DTA distributions is also difficult because of the general lack of experience that users have of their examination. The values in quadrant 1 are, as expected, 0 cm. The DTA in quadrant 2 is more complex, but some features can be identified. First, the DTA is almost zero near the steep dose gradient region, because even dose differences greater than 3% effectively shift the steep dose gradients less than 1 mm. In both the high and low dose regions where the dose gradient is shallow, the DTA increases rapidly as the dose difference increases, such that the DTA exceeds 1 cm (the maximum distance used for the DTA search algorithm) for dose differences of as small as 1%. Because most of the quadrant contains shallow dose gradient regions, most of the quadrant has large DTA values. The DTA in quadrant 3 exhibits a smooth increase in value as a function of the spatial offset, with a small decrease in the low-dose region near the diagonal divisions. The DTA in quadrant 4 shows a combination of the results of quadrants 2 and 3.

The color-wash in the composite distribution [Fig. 1(e)] shows the regions that pass either or both the dose-difference and DTA tests (blue) and fail both tests (red). In quadrant 1, the dose distributions were the same, so the entire area passed. In quadrant 2, the dose gradient exceeded the 3% criterion at 2.5 cm off-axis distance, so the comparison failed in regions lateral to ± 2.5 cm, except in regions of steep dose gradients, where the DTA was less than the 3 mm criterion. In quadrant 3, the position shift caused dose discrepancies that were much less than the 3% criterion in the shallow dose gradient regions. In the steep dose gradient regions, the spatial offsets between the two distributions were greater than 3

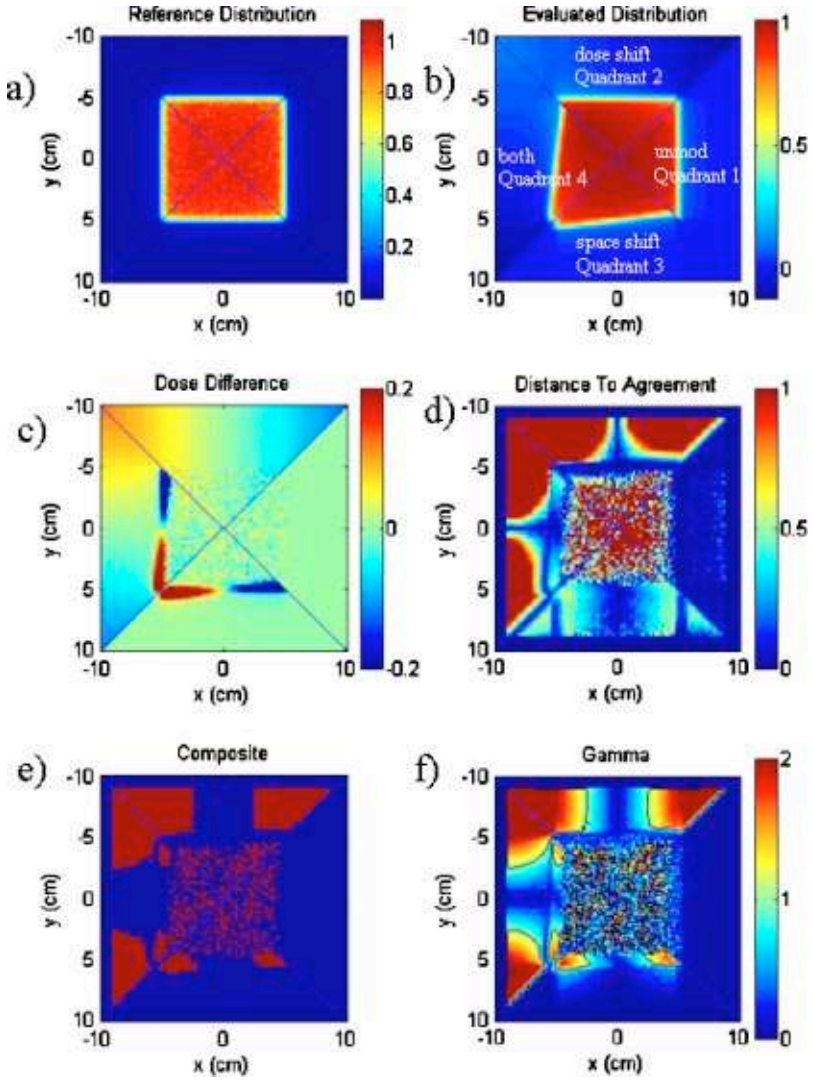

FIG. 2. Example of dose analysis tools for model and modified 10×10 cm^2 fields representing the reference and evaluated dose distributions, respectively, with 3% noise (multiplicative) added to the reference dose distribution. The gamma tool uses 3% and 3 mm dose difference and distance-to-agreement criteria, respectively.

mm lateral to ± 2.5 cm off-axis distance, so the composite distribution showed failure of both tests outside ± 2.5 cm. Similarly, in quadrant 4, both steep and shallow dose gradient regions failed outside the 2.5 cm region. While the composite distribution accurately identified regions that fail both criteria, it was only a pass-fail test and did not indicate by how much the distributions passed or failed.

The γ distribution is shown in Fig. 1(f). The $\gamma=1$ contour has been drawn to assist the comparison against the composite distribution. In all 4 quadrants, the regions that failed the γ-distribution test were nearly identical to the regions that failed the composite test. The advantage of using γ was that the comparison was a continuous function, so the magnitude of passing or failure was easily identified.

The influence of 3% standard deviation multiplicative pseudorandom noise on the reference distribution is shown in Fig. 2. The influence on the dose difference was straightforward and did not reduce the sensitivity of the dose difference on steep dose gradient regions [Fig. 2(c)]. The DTA distribution [Fig. 2(d)] was more profoundly affected by the noise. In the shallow dose gradient regions, the structure that was seen in Fig. 1(d) was disrupted by the noise, but in the steep dose gradient region, where the DTA was most useful, the DTA still measures the distance between the two dose distributions (quadrants 3 and 4). Similarly, for the composite distribution, the noise in the shallow dose gradient region caused the composite distribution to mimic the noise, but in steep dose gradients, where the noise had a relatively small effect on the DTA, the composite distribution was relatively unchanged. A very similar result was seen in the γ distribution, where for steep dose gradient regions, the γ distribution was relatively unaffected, but in shallow dose gradient regions, the γ distribution was profoundly affected by the noise.

A very different result was seen when 3% standard deviation normally distributed pseudorandom noise was added to the evaluated distribution (Fig. 3). The dose-difference distribution was essentially the same as when the noise was

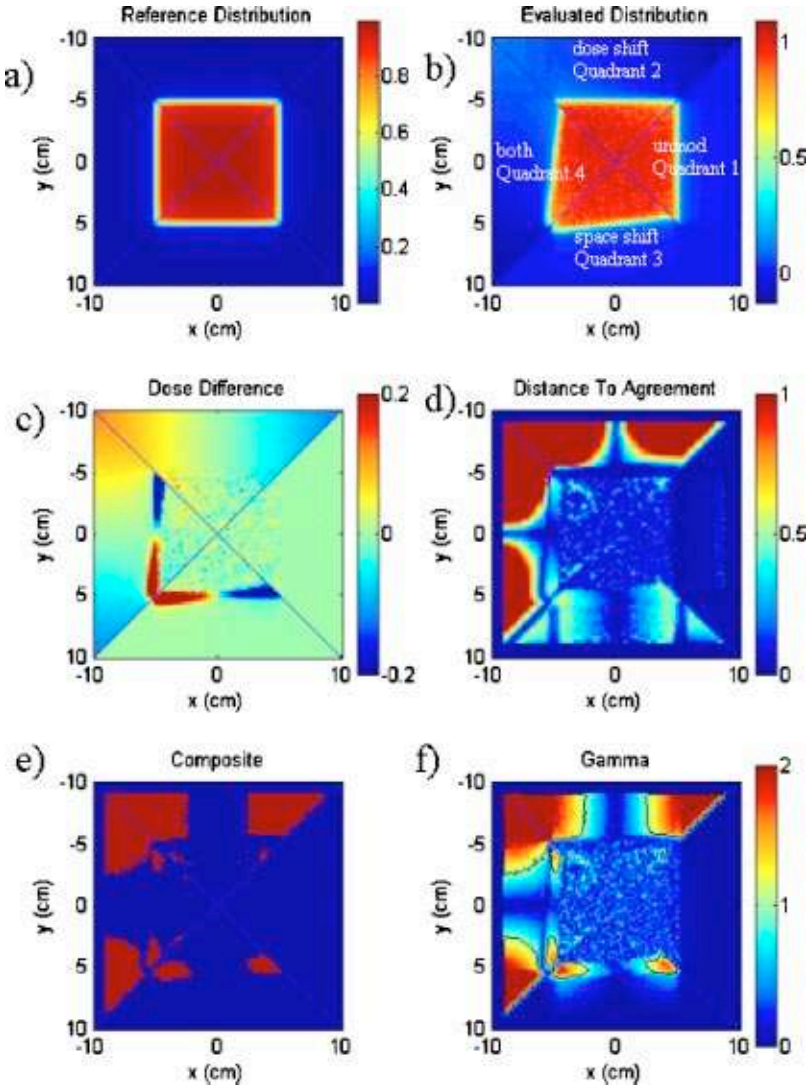

FIG. 3. Example of dose analysis tools for model and modified 10×10 cm^2 fields representing the reference and evaluated dose distributions, respectively, with 3% noise (multiplicative) addded to the evaluated dose distribution. The gamma tool uses 3% and 3 mm dose difference and distance-to-agreement criteria, respectively.

added to the reference distribution, but the DTA looked very different. Because the DTA was calculated on a point-by-point basis for the reference distribution, the effect of adding noise to the evaluated distribution was to provide opportunities to locate a point in the evaluated distribution that was closer than the DTA that would be determined with no noise. This could be seen in the high dose, shallow dose gradient regions of quadrants 2 and 4, where the DTA values were smaller than with no noise. The composite and γ distributions also reflected this result, with only very small portions of the steep dose regions that failed the composite or γ tests. This was in contrast with the no-noise case, where the regions near the field corners failed the comparisons based on dose differences greater than 3%.

B. Constant dose gradient

The constant gradient test results are shown in Figs. 4–6 using the same 3% and 3 mm criteria. The figures show two-dimensional distributions that are collections of γ histograms for a series of added noise standard deviations. The noise was added to the evaluated and reference distributions on the left and right columns, respectively. The first row in each figure represented the histogram in the absence of noise. Because these dose distributions were both constant and equal gradients, each reference point was the same distance from the evaluated distribution, so for no noise, they had the same value of γ and the histograms were single valued. The results shown in Fig. 4 compared the γ histograms for evaluated and reference dose distributions that differed by 6%, for dose gradients of 0, 10% cm^{-1}, and 50% cm^{-1}, corresponding to gradients experienced throughout clinical IMRT dose distributions. For 0% dose gradient [Figs. 4(a) and 4(b)], as the evaluated distribution noise increased, the average value of γ decreased almost linearly until reaching a minimum value, where it remained almost constant with increasing noise. As the gradient increased, the no-noise value of γ

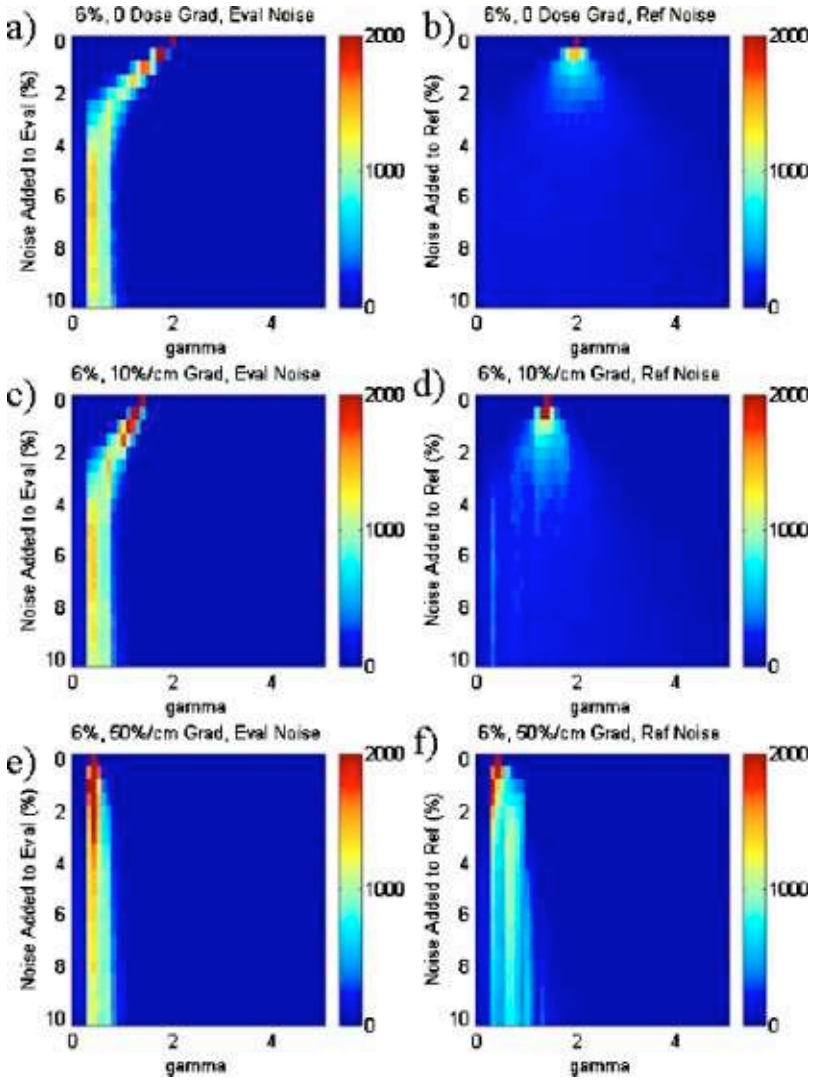

FIG. 4. Constant gradient tests showing the effect of noise on γ histograms (3%, 3 mm criteria) for three dose differences with noise added to the evaluated (a), (c), (e) and reference (b), (d), (g) distributions. The color scale indicates the number of histogram pixels.

decreased because the distance between the two distributions in the renormalized space decreased. Again, with noise added to the evaluated distribution, the value of γ decreased to an asymptotic value of approximately 0.33 at a noise level of 3%.

When noise was added to the reference distribution, the average value of γ changed very little, but the width of the γ distribution increased linearly with the added noise. For 0% gradient [Fig. 4(b)], the standard deviation of the γ distribution was equal to the standard deviation of the noise. The behavior was also seen for 10% cm^{-1} dose gradient. At 50% cm^{-1} the steep gradient over-rode the relatively small dose difference of 6%, and the γ-test degenerated to a DTA test. The DTA for a 6% dose difference in a 50% cm^{-1} dose gradient was 1.2 mm, equivalent to $\gamma=0.4$ with the selected criteria. In these conditions, the value of γ with no noise was small, and increasing noise broadened the γ histogram width slightly.

The effect of noise on a varying dose difference while maintaining a constant dose gradient (0%) is shown in Fig. 5. The no-noise histograms (the first rows) were, as expected peaked at $\gamma=0$, $\gamma=1$, and $\gamma=2$ for the 0%, 3%, and 6% dose differences. When noise was added to the evaluated distribution, the peak shifted linearly to an asymptotic value of $\gamma\cong0.33$ for all dose differences. When noise was added to the reference distribution the peak value remained constant, but the histogram broadened with a standard deviation equal to the standard deviation of the noise (after renormalization by the dose-difference criterion).

To examine the asymptotic behavior of noise as a function of pixel spacing, the simulation was repeated for a constant dose difference of 6% and no dose gradient, for 1 mm, 2 mm, and 3 mm pixel spacing (Fig. 6). The no-noise peak values were not altered by the change in pixel spacing because evaluated and reference dose distribution pixel locations were collocated. The asymptotic value of γ for noise added to the evaluated distribution shifted linearly with increased pixel spacing, corresponding to the pixel spacing divided by the distance criterion. For example, with a 3 mm pixel spacing and a 3 mm criterion, the asymptotic value of γ

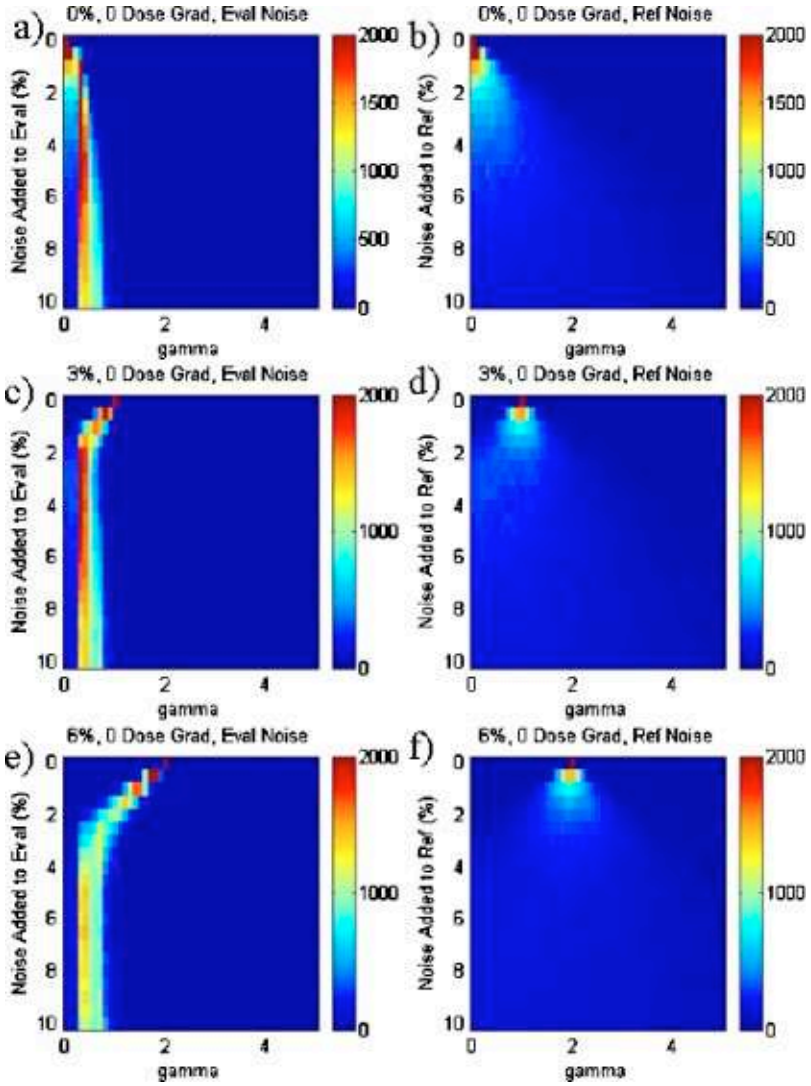

FIG. 5. Constant gradient tests showing the effect of noise on γ histograms (3%, 3 mm criteria) for three dose differences and no dose gradient with noise added to the evaluated (a), (c), (e) and reference (b), (d), (g) distributions. The color scale indicates the number of histogram pixels.

was approximately 1. Shifts in the histogram values of γ were linear up to the value of γ corresponding to the pixel spacing. As before, noise added to the reference distribution spread the γ histogram peak, but the mean value stayed relatively constant.

IV. DISCUSSION AND CONCLUSIONS

Recently, Depuydt *et al.*[18] published a clinical assessment of the γ tool, providing a review of the calculation technique and some examples of its use. They were concerned with errors in the γ calculation in steep dose gradient regions, and with the calculation time required to calculate γ. Instead, they determine if the γ value was greater or less than 1, rather than determining the value. This effectively reduced the γ tool to an equivalent of the composite evaluation, removing the continuous nature of γ. While we have seen artifacts in γ calculations owing to large evaluated dose distribution matrix spacings, interpolation to 1×1 mm^2 grids (as used in this paper) keep these artifacts to less than 0.2, even in steep dose gradient regions. For clinical cases, the calculation time is typically 5 minutes for a 1×1 mm^2 interpolated resolution on an 800 MHz Pentium 4 for a 14.1 $\times15.2$ cm^2 radiographic film.

We found that the dose evaluation tools provided a comprehensive, quantitative comparison between two dose distributions. For dose distribution overlays or dose-difference determinations, the results were independent to within a sign of selection of the reference or evaluated distribution. However, for the DTA and γ tools, the results could be profoundly affected by the selection, especially when one or both of the dose distributions contained some noise. Typically, the reference and evaluated distributions would refer to measured and calculated distributions, respectively, but the final selection should be based on which distribution is considered the standard by which the other is compared. Because the DTA and γ distributions were computed on a point-by-point basis for the reference distribution, it would typically be the distribution with the sparsest data and could even be conducted on a

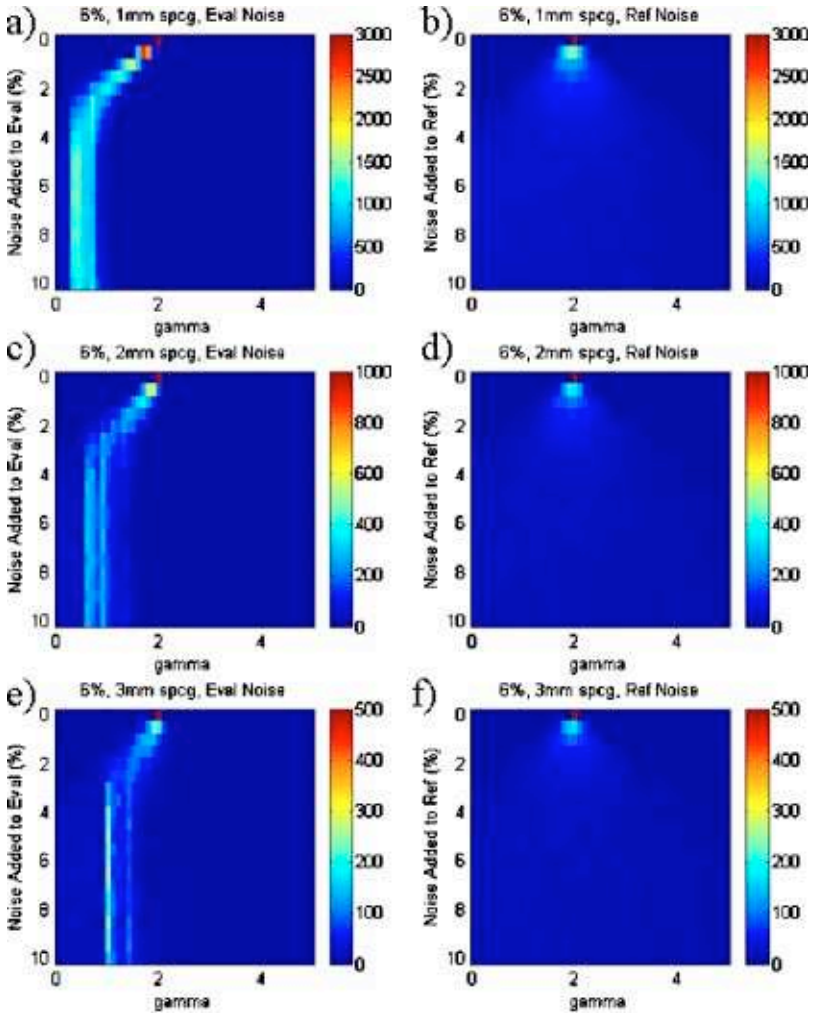

FIG. 6. Constant gradient tests showing the effect of noise on γ histograms (3%, 3 mm criteria) for 6% dose differences and no dose gradient as a function of dose distribution pixel spacing with noise added to the evaluated (a), (c), (e) and reference (b), (d), (g) distributions. The color scale indicates the number of histograms pixels.

single measurement point (e.g., an ionization chamber measurement). The effect of measurement or calculation noise (e.g., with Monte Carlo dose calculations) might also affect the selection of the reference or evaluated distributions.

The pixel spacing of the evaluated distribution needed to be sufficiently small to provide accurate calculations of γ in steep dose gradient regions. Without spatial interpolation, the values of γ in steep dose gradients could be in error, causing distracting artifacts in γ distributions. As a general rule, the spacing should be less than or equal to 1/3 of Δd. We are investigating a method for determining the maximum acceptable pixel spacing as a function of the local dose gradient and desired γ accuracy.

While the constant-gradient γ-histogram analysis showed significant perturbations in the presence of noise, the study was conducted with greater noise standard deviations than typically found in clinical cases. For nonstochastic dose calculations, the point-to-point variation should be less than the noise examined in this study. However, for the evaluation of Monte Carlo dose calculations, both the DTA and γ functions would be sensitive to noise. If the calculation was considered the evaluated distribution, it would underestimate the γ comparison. For example, in regions where the two dose distributions differ by only an average value of 3%, 1% standard deviation noise in the evaluated distribution would reduce the average value of γ from 1.0 to 0.5. This would make quantitative use of the γ distribution more difficult, because the acceptability of the comparison would need to consider not only ΔD and Δd, but also the expected pixel-to-pixel noise standard deviation. The situation would be different if the Monte Carlo calculation is considered the reference distribution. The average value of γ would be accurately calculated, but γ would vary point-by-point, so some smoothing of the γ distribution might be appropriate.

The γ distribution is a magnitude value and consequently has no numerical sign. It measures the closest distance between each reference point and evaluated dose distributions after scaling by ΔD and Δd. Because the γ tool involves the simultaneous evaluation of dose and distance dimensions, there as been some justifiable confusion regarding what the γ tool means. For example, does a common value of $\gamma=1$ have the same meaning in a steep or shallow gradient re-

gion? The computed value of γ is a measurement of the distance between the two dose distributions in the renormalized space. The vector corresponding to the shortest distance is, by definition, orthogonal to the evaluated distribution. The orientation of that vector relative to the spatial axes will be a function of the local dose gradient. The steeper the dose gradient, the more the γ vector is perpendicular to the dose axis and parallel to the spatial axes. As the dose gradient approaches infinity, the γ vector becomes perpendicular to the dose axis and is a direct measurement of the DTA. Conversely, for zero dose gradients, the vector is parallel to the dose axis and γ is a measure of the dose difference. Therefore, γ automatically accounts for the local gradient to select the proper test when comparing the distributions.

Another potential use of the γ distribution is to equate Δd criterion with spatial error bars in the dose distributions. In steep dose gradient regions, the dose difference is not significant relative to the spatial error bar, and the γ value is reduced by the spatial component of the γ vector. The γ distribution therefore shows the dose difference with consideration of the spatial error bars and the local dose gradient.

The γ tool provides a quantitative method for comparing two dose distributions. In this paper, we have shown the utility of the tool to compare two similar dose distributions and evaluated the sensitivity of the tool to pseudorandom noise. In all of these tests, the dose and distance criteria were fixed, preselected values. In practice, the values can be set as functions of space (the location of the dose comparison) or dose value. For example, near a critical structure boundary, the value of Δd may be reduced to highlight spatial errors in that region. Also, the dose difference criterion ΔD may be relaxed for low-dose regions or regions not in a critical structure or target. The application of γ with these added degrees of freedom is being investigated.

ACKNOWLEDGMENTS

This work was supported in part by a corporate grant from Computerized Medical Systems and by NIH R01 84409.

[a]Author to whom correspondence should be addressed; electronic mail: low@radonc.wustl.edu

[1] L. J. van Battum and B. J. Heijmen, "Film dosimetry in water in a 23 MV therapeutic photon beam," Radiother. Oncol. **34**, 152–159 (1995).
[2] J. F. Williamson, F. M. Khan, and S. C. Sharma, "Film dosimetry of megavoltage photon beams: A practical method of isodensity-to-isodose curve conversion," Med. Phys. **8**, 94–98 (1981).
[3] J. L. Robar and B. G. Clark, "The use of radiographic film for linear accelerator stereotactic radiosurgical dosimetry," Med. Phys. **26**, 2144–2150 (1999).
[4] J. I. Hale, A. T. Kerr, and P. C. Shragge, "Calibration of film for accurate megavoltage photon dosimetry," Med. Dosim. **19**, 43–46 (1994).
[5] M. D. Evans and L. J. Schreiner, "A simple technique for film dosimetry," Radiother. Oncol. **23**, 265–267 (1992).
[6] C. Danciu, B. S. Proimos, J. C. Rosenwald, and B. J. Mijnheer, "Variation of sensitometric curves of radiographic films in high energy photon beams," Med. Phys. **28**, 966–974 (2001).
[7] A. Ertl, A. Berg, M. Zehetmayer, and P. Frigo, "High-resolution dose profile studies based on MR imaging with polymer BANG(TM) gels in stereotactic radiation techniques," Magn. Reson. Imaging **18**, 343–349 (2000).
[8] D. A. Low, J. F. Dempsey, R. Venkatesan, S. Mutic, J. Markman, E. Mark Haacke, and J. A. Purdy, "Evaluation of polymer gels and MRI as a 3-D dosimeter for intensity-modulated radiation therapy," Med. Phys. **26**, 1542–1551 (1999).
[9] D. A. Low, J. Markman, J. F. Dempsey, S. Mutic, M. Oldham, R. Venkatesan, E. M. Haacke, and J. A. Purdy, "Noise in polymer gel measurements using MRI," Med. Phys. **27**, 1814–1817 (2000).
[10] M. J. Maryanski, J. C. Gore, R. P. Kennan, and R. J. Schulz, "NMR relaxation enhancement in gels polymerized and cross-linked by ionizing radiation: a new approach to 3D dosimetry by MRI," Magn. Reson. Imaging **11**, 253–258 (1993).
[11] M. J. Maryanski, R. J. Schulz, G. S. Ibbott, J. C. Gatenby, J. Xie, D. Horton, and J. C. Gore, "Magnetic resonance imaging of radiation dose distributions using a polymer gel dosimeter," Phys. Med. Biol. **39**, 1437–1455 (1994).
[12] M. J. Maryanski, G. S. Ibbott, P. Eastman, R. J. Schulz, and J. C. Gore, "Radiation therapy dosimetry using magnetic resonance imaging of polymer gels," Med. Phys. **23**, 699–705 (1996).
[13] M. Oldham, I. Baustert, C. Lord, T. A. Smith, M. McJury, A. P. Warrington, M. O. Leach, and S. Webb, "An investigation into the dosimetry of a nine-field tomotherapy irradiation using BANG-gel dosimetry," Phys. Med. Biol. **43**, 1113–1132 (1998).
[14] A. Appleby, E. A. Christman, and A. Lefhrouz, "Imaging of spatial radiation dose distribution in agarose gels using magnetic resonance," Med. Phys. **14**, 382–384 (1987).
[15] W. B. Harms, D. A. Low, J. W. Wong, and J. A. Purdy, "A software tool for the quantitative evaluation of 3D dose calculation algorithms," Med. Phys. **25**, 1830–1836 (1998).
[16] D. A. Low, W. B. Harms, S. Mutic, and J. A. Purdy, "A technique for the quantitative evaluation of dose distributions," Med. Phys. **25**, 656–661 (1998).
[17] J. Van Dyk, R. B. Barnett, J. E. Cygler, and P. C. Shragge, "Commissioning and quality assurance of treatment planning computers," Int. J. Radiat. Oncol., Biol., Phys. **26**, 261–273 (1993).
[18] T. Depuydt, A. V. Esch, and D. P. Huyskens, "A quantitative evaluation of IMRT dose distributions: refinement and clinical assessment of the gamma evaluation," Radiother. Oncol. **62**, 309–319 (2002).
[19] A. S. Shiu, S. Tung, K. R. Hogstrom, J. W. Wong, R. L. Gerber, W. B. Harms, J. A. Purdy, R. K. TenHaken, D. L. McShan, and B. A. Fraass, "Verification data for electron beam dose algorithms," Med. Phys. **19**, 623–636 (1992).
[20] A. Cheng, W. B. Harms, R. L. Gerber, J. W. Wong, and J. A. Purdy, "Systematic verification of a three-dimensional electron beam dose calculation algorithm," Med. Phys. **23**, 685–693 (1996).
[21] K. T. Islam, J. F. Dempsey, M. K. Ranade, M. Maryanski, and D. A. Low, "Initial evaluation of a commercial optical CT-based scanner for 3D gel dosimetry," Med. Phys. (in press).
[22] J. J. DeMarco, T. D. Solberg, and N. Agazaryan, "A seed specific dose kernel method for low-energy brachytherapy dosimetry," J. Appl. Clinc. Med. Phys. **4**, 66–74 (2003).
[23] N. Agazaryan, T. D. Solberg, and J. J. DeMarco, "Patient specific quality assurance for the delivery of intensity modulated radiotherapy," J. Appl. Clinc. Med. Phys. **4**, 40–50 (2003).